JCB Article

Pheromone-induced polarization is dependent on the Fus3p MAPK acting through the formin Bni1p

Dina Matheos,[1] Metodi Metodiev,[2] Eric Muller,[1] David Stone,[2] and Mark D. Rose[1]

[1]Department of Molecular Biology, Princeton University, Princeton, NJ 08544
[2]Department of Biological Sciences, University of Illinois-Chicago, Chicago, IL 60607

During mating, budding yeast cells reorient growth toward the highest concentration of pheromone. Bni1p, a formin homologue, is required for this polarized growth by facilitating cortical actin cable assembly. Fus3p, a pheromone-activated MAP kinase, is required for pheromone signaling and cell fusion. We show that Fus3p phosphorylates Bni1p in vitro, and phosphorylation of Bni1p in vivo during the pheromone response is dependent on Fus3p. *fus3* mutants exhibited multiple phenotypes similar to *bni1* mutants, including defects in actin and cell polarization, as well as Kar9p and cytoplasmic microtubule localization. Disruption of the interaction between Fus3p and the receptor-associated Gα subunit caused similar mutant phenotypes. After pheromone treatment, Bni1p-GFP and Spa2p failed to localize to the cortex of *fus3* mutants, and cell wall growth became completely unpolarized. Bni1p overexpression suppressed the actin assembly, cell polarization, and cell fusion defects. These data suggest a model wherein activated Fus3p is recruited back to the cortex, where it activates Bni1p to promote polarization and cell fusion.

Introduction

Saccharomyces cerevisiae reproduces sexually, through mating and meiosis (for review see Sprague and Thorner, 1994; Marsh and Rose, 1997). Haploid yeast cells exist in two mating types, *MAT***a** and *MAT*α, which secrete mating type–specific peptide pheromones that bind to specific transmembrane receptor proteins on the opposite cell type. When either cell is stimulated by pheromone, an intracellular signal transduction cascade is initiated that leads to a switch in the growth pattern from budding to mating. Stimulated cells polarize their growth toward each other, forming elongated projections following the pheromone gradient until cells have come into contact. Cells with mating projections are often referred to as "shmoos." After contact, a stable junction is formed between the mating pair such that the intervening cell walls can be safely degraded and the plasma membranes can fuse. After cell fusion, the two haploid nuclei move toward each other and fuse to form a single diploid nucleus. The diploid zygotic cell then reenters the mitotic cell cycle.

Several proteins are required for cell fusion, including the MAPK, Fus3p. Although its specific role in cell fusion is unclear, Fus3p has several well-characterized functions in signal transduction and pheromone-induced cell cycle arrest (Elion et al., 1990; Fujimura, 1990). After pheromones bind to their receptor (Ste2p or Ste3p, depending on mating type), the associated trimeric G protein dissociates into Gα and Gβγ subunits (Gpa1p, Ste4p, and Ste18p, respectively). Free Gβγ interacts with several proteins, including Ste20p, a p21-activated protein kinase, and Ste5p, a scaffolding protein for the MAPK cascade comprised of Ste11p, Ste7p, and Fus3p. Ste20p phosphorylates Ste11p, which phosphorylates Ste7p, which phosphorylates and activates Fus3p. Activated Fus3p then enters the nucleus where it phosphorylates Dig1p and Dig2p, negative regulators of the transcription factor Ste12p, leading to the transcription of genes required for cell and nuclear fusion (Cook et al., 1997; Tedford et al., 1997). In some strains, Fus3p is not essential for transcriptional activation because of the presence of a second partially redundant MAPK, Kss1p (Elion et al., 1991a,b). Activated Fus3p also phosphorylates Far1p (Elion et al., 1993), which acts as a cell cycle inhibitor to arrest the cell in G1. The requirement for Fus3p in cell cycle arrest can be suppressed by deletion of the G1 cyclin, *CLN3* (Elion et al., 1990).

Far1p plays a second role in determining the site of cell polarization (Valtz et al., 1995). In mitosis, Far1p is resident

Address correspondence to Mark Rose, Dept. of Molecular Biology, Princeton University, Princeton, NJ 08544-1014. Tel.: (609) 258-2804. Fax: (609) 258-1975. email: mrose@molbio.princeton.edu

Key words: yeast; mating; actin; cytoskeleton; signal transduction

Abbreviation used in this paper: 1-Na PP1, 1-napthyl PP1.

The Journal of Cell Biology, Volume 165, Number 1, April 12, 2004 99–109
http://www.jcb.org/cgi/doi/10.1083/jcb.200309089

The Journal of Cell Biology

in the nucleus, where it sequesters Cdc24p, the exchange factor for the Rho-like G protein, Cdc42p. Cell cycle–dependent degradation of Far1p allows the release and recruitment of Cdc24p to the incipient bud (Shimada et al., 2000). However, during mating, a Far1p–Cdc24p complex exits the nucleus and interacts with Gβγ at the cortex, recruiting Cdc42p and Bem1p away from the bud site (Butty et al., 1998; Nern and Arkowitz, 1999). Mutants lacking Far1p still form shmoos, which are mislocalized at the site of bud emergence, rather than toward the mating partner. These results suggest that Far1p is required for orienting the shmoo projection, but not for the intrinsic mechanism of polarization. Mutants in which both the bud site and Far1p-dependent orientation have been inactivated show residual polarization, implying that there is another pathway responsible for pheromone-induced polarization (Nern and Arkowitz, 2000a).

Mutations in *fus3* cause a profound cell fusion defect (Elion et al., 1990), and several lines of evidence suggest that the cell fusion defect may be independent of defects in transcriptional activation and cell cycle arrest. If the transcriptional activation defect is suppressed by overexpression of *STE12*, or if the cell cycle arrest defect is suppressed by deletion of *cln3* (Elion et al., 1991b; Fujimura, 1992), either singly (Elion et al., 1991b; Fujimura, 1992) or together (Matheos, 2003), *fus3* mutants still exhibit a strong cell fusion defect. Therefore, it is likely that Fus3p has additional functions that are required for cell fusion.

Mutations in several genes involved in polarity establishment exhibit cell fusion defects. In particular, mutations affecting proteins in the "polarisome" (Bni1p, Spa2p, and Pea2p) cause strong cell fusion defects (Gehrung and Snyder, 1990; Chenevert et al., 1994; Dorer et al., 1997; Evangelista et al., 1997; Gammie et al., 1998). Of particular interest is the formin protein, Bni1p. Formins regulate actin and cell polarization in response to a variety of stimuli in a wide variety of eukaryotes. Recently, Bni1p has been shown to facilitate actin cable polymerization in vitro (Evangelista et al., 2002; Pruyne et al., 2002; Sagot et al., 2002a,b). Bni1p interacts with Spa2p and Pea2p, and Spa2p is required for proper Bni1p localization to sites of polarized growth during mitosis (Fujiwara et al., 1998; Ozaki-Kuroda et al., 2001). Bni1p also interacts with and is regulated by a variety of rho-like G proteins (Dong et al., 2003). In particular, the small GTP-binding protein Cdc42p is known to regulate Bni1p function in both mitotic and mating cells to promote polarization (Evangelista et al., 1997). Because Cdc42p also interacts with Gβγ after release by the Gα subunit in response to pheromone (Butty et al., 1998; Nern and Arkowitz, 1999), it seems likely that this interaction plays a key role in the pathway by which cells polarize toward the pheromone gradient. Bni1p activated by Cdc42p near the site of pheromone response would nucleate actin cables, leading to polarized growth. Polarization is thought to be required during cell fusion to deliver proteins required for cell wall degradation and plasma membrane fusion (Gammie et al., 1998). In this paper, we provide evidence that one of Fus3p's functions during mating is the activation and localization of Bni1p, to promote cell polarization and cell fusion.

Results

Fus3p phosphorylates Bni1p

To identify substrates of the MAPK Fus3p required for cell fusion, we screened proteins to see if any could be phosphorylated by Fus3p in vitro. Fus3p copurifies with other kinases, including Ste11p and Ste7p (Choi et al., 1994), and Fus3p must be phosphorylated in response to pheromone to be fully active (Gartner et al., 1992). To assay Fus3p's protein kinase activity in the presence of other copurifying protein kinases, we used a form of the kinase engineered to use a novel ATP analogue, in addition to ATP. The bulky phenethyl-ATP is sterically hindered from binding to the acceptor pocket in the active site of most kinases. In previous work, Fus3p was engineered by introducing a single amino acid substitution (glutamine 93 to glycine) predicted to allow phenethyl-ATP to bind and serve as a phosphate donor (Shah et al., 1997; Liu et al., 1998; Bishop et al., 2000). Previously, we showed that Fus3p^{Q93G} activity in vivo (but not that of wild-type Fus3p) is inhibited by the cognate analogue of a protein kinase inhibitor, 1-napthyl PP1 (1-Na PP1), which has been modified with a similar bulky adduct (Bishop et al., 2000). To assay Fus3p activity, we partially purified either FLAG-tagged wild-type Fus3p or FLAG-tagged analogue-sensitive Fus3p^{Q93G} from mitotic or pheromone-induced extracts. Addition of [^{32}P]phenethyl-ATP to Fus3p^{Q93G} purified from pheromone-induced cells lead to a high level of phosphorylation of Fus3p and copurifying proteins (Fig. 1 A). Very little activity was observed with Fus3p^{Q93G} from uninduced mitotic cells or with wild-type Fus3p from either induced or mitotic cells. The residual activity observed with wild-type Fus3p from induced cells was effectively competed with excess ATP, whereas the activity observed with Fus3p^{Q93G} was refractory to competition. In contrast, the activity of Fus3p^{Q93G} was almost completely abolished by the addition of the analogue inhibitor 1-Na PP1, previously shown to inhibit the Fus3p^{Q93G} activity in vivo (Bishop et al., 2000; Metodiev et al., 2002). Similar results were observed for the phosphorylation of an exogenous protein substrate, myelin basic protein (MBP; Fig. 1 B). Using [^{32}P]phenethyl-ATP, phosphorylation was observed only with Fus3p^{Q93G} and was inhibited by 1-Na PP1. Together, these results demonstrate that the protein kinase assay is specific for the pheromone-activated form of the analogue-sensitive Fus3p^{Q93G}.

Next, we examined the ability of Fus3p^{Q93G} to phosphorylate proteins in a genomic library of GST fusion proteins (Martzen et al., 1999; Matheos, 2003). Known substrates of Fus3p (Dig1p and Dig2p) were among the proteins identified. We also examined the ability of Fus3p^{Q93G} to phosphorylate HA epitope–tagged proteins known to have a role in cell fusion, including Bni1p, Rvs161p, and Fus2p. Of these, only Bni1p was phosphorylated by Fus3p^{Q93G} in vitro (Fig. 1 C; unpublished data).

To validate the significance of the phosphorylation, we determined whether Bni1p is phosphorylated during mating in vivo, dependent upon Fus3p. Wild-type and *fus3*Δ cells were induced with pheromone and labeled with [^{32}P]orthophosphate. HA epitope–tagged Bni1p was immunoprecipitated and examined for the incorporation of ^{32}P (Fig. 1 C). In the wild type, a doublet of ^{32}P-labeled Bni1p proteins was

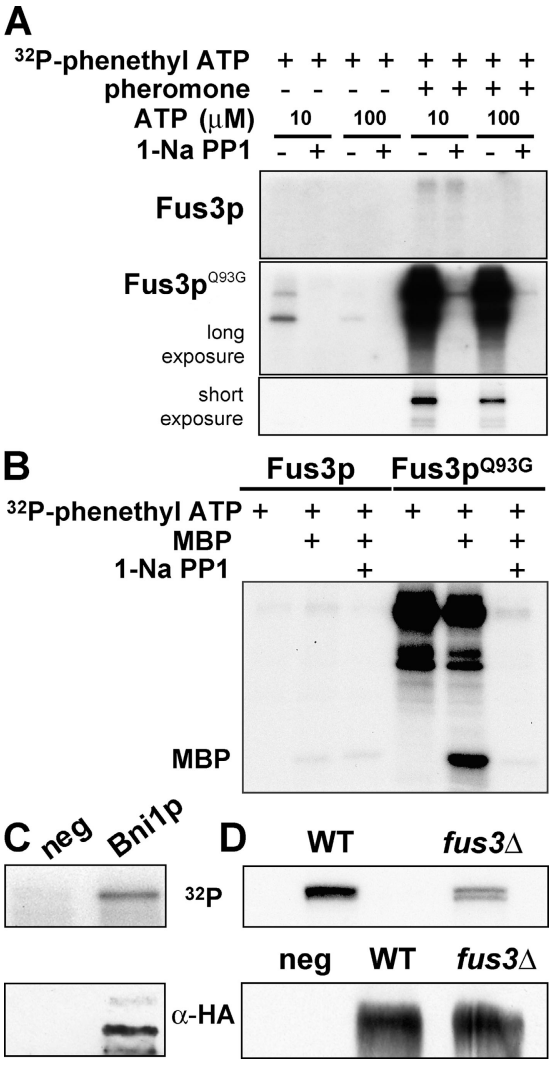

Figure 1. **Fus3p phosphorylates Bni1p both in vitro and in vivo.** (A) Wild-type FLAG-Fus3p and analogue-sensitive FLAG-Fus3p^{Q93G} were immunoprecipitated from mitotic and pheromone-induced extracts, and in vitro kinase assays were performed as described in the Materials and methods. Nonradioactive ATP was added to the indicated concentrations as a competitive inhibitor of endogenous kinases. The inhibitor analogue 1-Na PP1 was added to 5 μM in indicated lanes. The Fus3p panel and the top Fus3p^{Q93G} panel were exposed to x-ray film for equivalent times; the bottom Fus3p^{Q93G} panel shows a shorter exposure to allow visualization of individual protein bands. (B) Wild-type FLAG-Fus3p or inhibitor-sensitive FLAG-Fus3p^{Q93G} was immunoprecipitated from pheromone-induced extracts, and kinase assays were performed as described for A. Myelin basic protein (MBP) was added as an exogenous substrate. 1-Na PP1 was added to 10 μM in indicated lanes. (C) In vitro phosphorylation of Bni1p by Fus3p. Top: HA-Bni1p was immunoprecipitated out of yeast and added to FLAG-Fus3p^{Q93G} in the in vitro kinase assay. Bottom: Western blots were performed using anti-HA antibody (12CA5 at 1:2,500 dilution) to identify HA-Bni1p. In both cases, a strain containing no HA tagged proteins (EY699) was used as negative control. (D) In vivo phosphorylation of Bni1p is partially dependent on Fus3p. Top: wild-type (MY8195) and *fus3*Δ (MY8196) overexpressing HA-*BNI1* were induced with α-factor pheromone and labeled with [^{32}P]orthophosphate before immunoprecipitation as described in the Materials and methods. Bottom: cells treated under the same conditions were processed for Western blot analysis to determine total amount of protein immunoprecipitated from each strain. EY699 was used as the negative control.

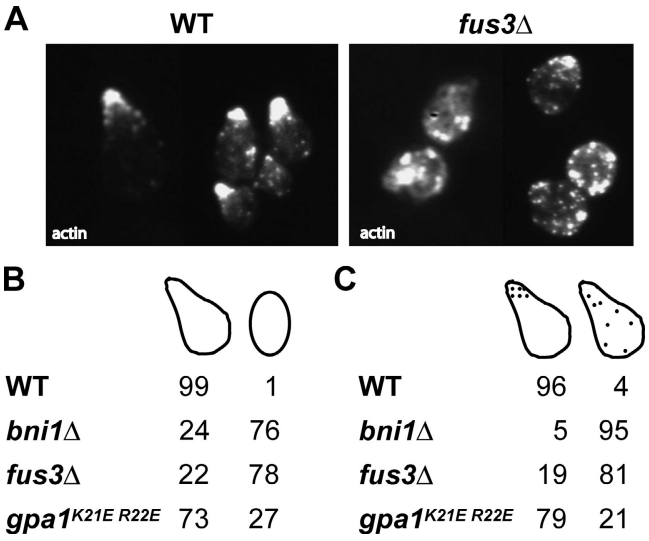

Figure 2. ***fus3* mutants have mislocalized actin and fail to polarize in response to pheromone.** (A) Cells were treated for 2.5 h with α-factor, fixed, and stained with rhodamine-phalloidin to examine actin localization by fluorescence microscopy as described in the Materials and methods. (B) WT (EY699), *bni1*Δ (MY8188), *fus3*Δ (EY700), and *gpa1*$^{K21E\ R22E}$ (MY8193) were scored for their ability to form shmoos after 1.5 h of exposure to pheromone ($n > 100$). (C) Cells were scored for their actin localization phenotype by fluorescence microscopy ($n > 100$).

observed with the top band containing a much higher level of incorporation. In the *fus3*Δ strain, incorporation of ^{32}P into the top band was severely reduced. The residual incorporation of ^{32}P into Bni1p in the *fus3*Δ strain is most likely due to mitotic phosphorylation (Goehring et al., 2003). In parallel control experiments, the total amount of protein purified from the wild-type and *fus3*Δ strains was found to be equal (Fig. 1 D). These data confirm that Bni1p is phosphorylated during the pheromone response in vivo, and that a portion of the phosphorylation is dependent on Fus3p.

*fus3*Δ mutants are defective in polarized morphogenesis and actin localization

Bni1p has several well-characterized roles in polarizing the actin cytoskeleton. Bni1p and the related formin Bnr1p are required for bud emergence during mitosis (Imamura et al., 1997), and Bni1p is required for shmoo formation in response to pheromone (Evangelista et al., 1997). During mating, *bni1* mutants fail to polarize, remain ellipsoidal, and contain delocalized cortical actin patches.

To determine whether Fus3p phosphorylation is required for Bni1p function, we examined *fus3* mutants for *bni1*-like phenotypes. First, we examined the morphology of cells responding to pheromone. Within 90 min of pheromone treatment, 99% of wild-type cells formed shmoo projections. In the same time, 76% of *bni1* mutant cells were unpolarized and remained ellipsoidal. Likewise, 78% of the *fus3* mutant cells were unpolarized (Fig. 2 B). Although most cells were rounded, a few partially polarized shmoo-like cells were observed among the *fus3*Δ cells, suggesting that hypophosphorylated Bni1p retains some function. Interestingly, most cells with shmoo-like morphology ap-

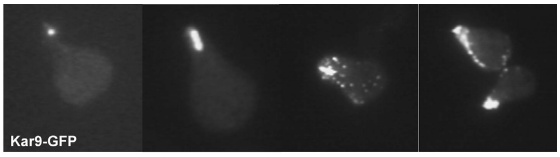

WT	84	10		6
***bni1*Δ**	28	20	12	40
***FUS3*^{Q93G}**	78	13		9
***FUS3*^{Q93G}** *+ 1-Na PP1*	13	31	20	36
***gpa1*$^{K21E\ R22E}$**	9	11	30	50

Figure 3. **Both *fus3* mutants and *gpa1*$^{K21E\ R22E}$ mutants mislocalize Kar9p.** Cells containing p*GAL-GFP-KAR9* were pregrown in raffinose, induced for 2 h by addition of galactose, and then pheromone was added for another 3 h. After brief fixation, *WT* (MY8189), *bni1*Δ (MY), *fus3-Q93G* (MY7494), and *gpa1*$^{K21E\ R22E}$ (MY8194) cells were scored for GFP-Kar9p localization ($n > 100$). To inactivate Fus3p^{Q93G} in vivo, 10 μM 1-Na PP1 was added after 60 min of pheromone induction. An equivalent amount of DMSO was added to a separate culture as a control. Cells were scored as having (from left to right): a single cortical dot, a line of localization, multiple dots near the shmoo tip, and dispersed dots elsewhere in the cell body, possibly on misoriented microtubules.

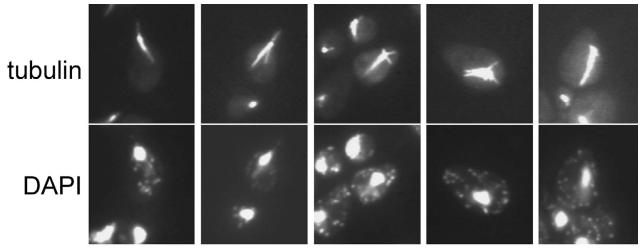

WT	91	4	5	0	0
***bni1*Δ**	14	23	23	37	6
***fus3*Δ**	35	2	8	56	0
***gpa1*$^{K21E\ R22E}$**	44	16	18	12	10
***fus3*Δ [*BNI1*]**	43	17	9	24	6

Figure 4. **Both *fus3* and *gpa1*$^{K21E\ R22E}$ mutants have misaligned microtubules.** WT (EY699), *bni1*Δ (MY8188), *fus3*Δ (EY700), *gpa1*$^{K21E\ R22E}$ (MY8193), and *fus3* p*GAL-BNI1* (MY8196) cells were induced with pheromone for 3 h and processed for immunofluorescence. Microtubules were detected with YOL1/34 as the primary antibody and the nucleus was stained with DAPI ($n > 100$). Cells were scored as having (from left to right): a single bundle of cytoplasmic microtubules going to the shmoo tip, a single bundle of cytoplasmic microtubules going to the shmoo tip plus other additional bundles oriented away from the shmoo tip, a spray of microtubules going to the shmoo tip, no cytoplasmic microtubules going to the shmoo tip, and long nuclear microtubules with short or nonexistent cytoplasmic microtubules.

peared to be buds that had begun to shmoo. Similar cells were not observed in the *bni1* mutant. The shmoo buds suggest that in the absence of Fus3p, the lack of cell cycle arrest allows residual polarization to occur from the bud site.

Next, we examined actin localization (Fig. 2, A and C). Although most wild-type cells (96%) showed a heavy concentration of actin at the shmoo tip (Fig. 2 A), actin patches were delocalized in the *fus3*Δ mutant cells (81%, Fig. 2 C). This defect was similar to that of the *bni1* mutant, in which 95% of cells showed actin delocalization. Because only partially polarized cells were counted to determine actin localization, the overall actin localization defect was more severe than these data indicate.

Phosphorylated Fus3p binds to activated Gpa1p, and the *gpa1*$^{K21E\ R22E}$ form of G_α is defective for binding to Fus3p in vivo (Metodiev et al., 2002). The *gpa1*$^{K21E\ R22E}$ mutant cells respond to pheromone, but their chemotropic response is compromised (Metodiev et al., 2002). We examined whether the interaction of Fus3p with Gpa1p might have a role in the activation of Bni1p. We found that the *gpa1*$^{K21E\ R22E}$ mutants were partly defective for actin polarization to the shmoo tip (21%) and for shmoo formation (27%; Fig. 2, B and C). These results suggest that the loss of the Gpa1p interaction may affect the efficiency of Fus3p regulation.

fus3 mutants do not localize Kar9p to the shmoo tip properly

Kar9p's localization to the shmoo tip is dependent on Bni1p and actin (Lee et al., 1999; Miller et al., 1999), presumably through the association of Kar9p and Myo2p with actin cables (Yin et al., 2000; Hwang et al., 2003). Therefore, we tested whether a *fus3* mutant would localize Kar9p properly (Fig. 3). Because shmoo-like cells are rare in the *fus3*Δ mutant, we used 1-Na PP1 to inactivate Fus3p^{Q93G} after cells had begun to polarize in response to pheromone. The *fus3-Q93G* strain was induced with pheromone for 60 min, after which 1-Na PP1 was added and incubated for an additional 30 min. As a control, a parallel culture of the *fus3-Q93G* strain was mock treated with DMSO. As expected, in the control cells, GFP-Kar9p was localized most frequently as a dot at the shmoo tip; a minor class of cells exhibited a line emanating from the shmoo tip (Lee et al., 1999; Miller et al., 1999). In cells treated with 1-Na PP1, Kar9p was delocalized to multiple dots at the shmoo tip (20%) or to dots throughout the cell body (36%). This phenotype was very similar to that of *bni1* mutants (Lee et al., 1999; Miller et al., 1999). The *gpa1*$^{K21E\ R22E}$ mutant showed an even stronger defect in Kar9p localization, with 80% of shmoos showing mislocalized Kar9p.

Because Kar9p is required for their normal localization to the shmoo tip (Miller et al., 1999), we next examined the cytoplasmic microtubules (Fig. 4). In the wild type, 95% of cells exhibited a single bundle of microtubules oriented to the shmoo tip, and a few cells contained a spray of microtubules reaching to the shmoo tip. No cells had completely misaligned microtubules. As previously reported, most *bni1*

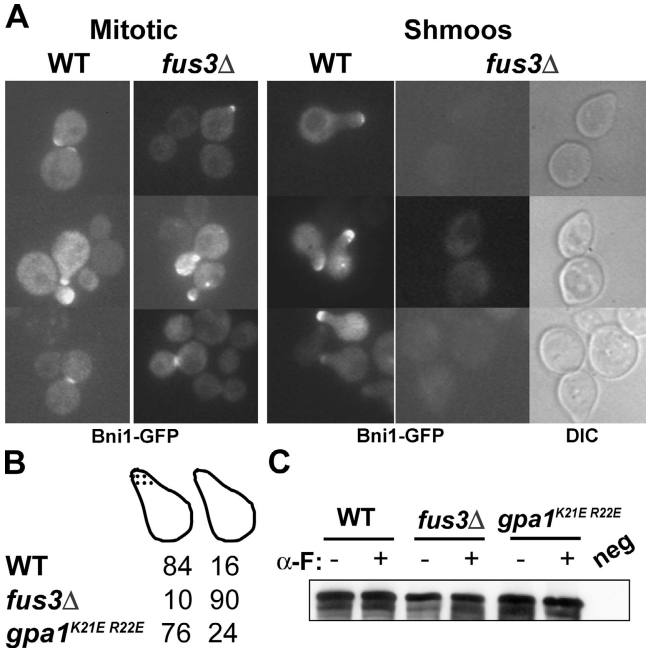

Figure 5. **Bni1p is not localized properly in shmoos in a *fus3* mutant.** (A) *WT* (MY8195), *fus3*Δ (MY8196), and *gpa1*$^{K21E\ R22E}$ (MY) strains containing *pGAL-BNI1-GFP* were grown in the presence of galactose for 2 h and then split into two cultures either with or without the addition of pheromone for an additional 2 h. Cells were fixed briefly with formaldehyde and examined by fluorescence microscopy. For *fus3* mutants, a brightfield image of the cells is also shown to indicate the outline of the cell. (B) Quantification of Bni1p localization in the strains ($n > 200$). (C) Total Bni1p was monitored by Western blots on extracts from cultures treated in the same way as for the microscopy. 12CA5 anti-HA antibody was used to detect Bni1p.

cells showed microtubule orientation defects, with only 37% of cells having a single bundle of microtubules going into the shmoo tip. There was a significant increase in the number of cells with splayed microtubules (23%) or severely misoriented microtubules (37%) that were not oriented near the shmoo tip. A similar result was seen for the *fus3* mutant cells, except that the class with completely misoriented microtubules increased to 56% (Fig. 4). The *gpa1*$^{K21E\ R22E}$ mutant cells also exhibited an increase in the number of cells with splayed microtubules in the shmoo tip and with severely misaligned microtubules. Therefore, these three mutants have similar effects in cytoplasmic microtubule orientation, which may result from the inability to localize Kar9p properly to the shmoo tip.

Fus3p is required for Bni1p localization to the shmoo tip

Next, we examined whether Fus3p phosphorylation is required for Bni1p localization. For this purpose, we expressed a fully functional HA-Bni1p-GFP construct in wild-type, *fus3*Δ, and *gpa1*$^{K21E\ R22E}$ cells (Evangelista et al., 1997). Bni1p colocalizes with actin at cortical sites where cell growth and secretion occur. As previously observed, in both wild-type and *fus3*Δ mitotic cells, Bni1p was localized to the incipient bud site, the tip of the growing bud, and the mother-bud neck at cytokinesis. Bni1p was found at the shmoo tip in 84% of wild-type cells treated with pheromone (Fig. 5 A). In contrast, Bni1p was localized in only 10% of the *fus3*Δ cells treated with pheromone. HA-Bni1p-GFP localization was not detected either by direct visualization or by indirect immunofluorescence (Fig. 5, A and B). HA-Bni1p-GFP localized normally in a strain deleted for *KSS1* (unpublished data), indicating that the defect is specific to *fus3*. The *gpa1*$^{K21E\ R22E}$ mutant also showed a partial loss of Bni1p localization at the shmoo tip (26%), consistent with the partial defect in actin polarization and shmoo formation. Loss of localization was not due to defects in the expression or stability of Bni1p (Fig. 5 C).

To confirm the requirement for Fus3p's kinase activity, we examined the localization of Bni1-GFP in the *fus3-Q93G* mutant. By 90 min of pheromone induction, almost all (>90%) of the cells formed shmoos and Bni1-GFP was properly localized (86%). Subsequent treatment with 1-Na PPi (60 min) caused mislocalization of Bni1-GFP in the majority of cells (58%), and the localized Bni1p-GFP was substantially dimmer. 1-Na PP1 had no effect in *FUS3* wild-type cells. When 1-Na PP1 was added with pheromone, by 2.5 h very few (16%) of the *fus3-Q93G* mutants formed shmoos, and Bni1-GFP was mislocalized in most (73%), similar to the *fus3*Δ mutant. In contrast, almost all (>90%) of wild-type cells formed shmoos, and Bni1-GFP was properly localized in most (79%). Because the level of Fus3p-Q93G is unaffected by 1-Na PP1 (Matheos, 2003), these results support the hypothesis that Fus3p's kinase activity is required to localize Bni1p.

Because Bni1p interacts with components of the polarisome (Fujiwara et al., 1998; Sheu et al., 2000), we next examined the localization of GFP-Spa2p. Normally, Spa2p localizes to the shmoo tip (Fig. 6 A). In contrast, in both *bni1* and *fus3* mutant cells, 92% and 88% of cells, respectively, showed no localization of Spa2p at the shmoo tip. These results show that Fus3p is required for the polarized localization of the polarisome during mating.

Overexpression of Bni1p suppresses a *fus3*Δ mutant strain

If Fus3p's role in polarization and cell fusion is through Bni1p, then Fus3p-independent activation of Bni1p should partially suppress the requirement for Fus3p. As predicted, overexpression of Bni1p-GFP from the *GAL1* promoter partially suppressed the polarization defect. Although only 22% of *fus3*Δ mutants were able to shmoo, upon Bni1p overexpression 69% of cells polarized in response to pheromone (Fig. 7, A and C). Furthermore, although only 18% of *fus3*Δ shmoos had polarized actin, overexpression of Bni1p-GFP caused 50% of cells to localize actin to the shmoo tip (Fig. 7 B). Consistent with these data, the overexpression of Bni1p-GFP also partially suppressed misorientation of the cytoplasmic microtubules (Fig. 4).

Although actin was polarized in these cells, its localization was often noticeably different from the wild type. Wild-type shmoos invariably contained a single projection with actin concentrated at the cortex. Although wild-type cells exposed to mating pheromone for longer times produce additional shmoo projections, only one projection will contain cortical actin patches. In contrast, in 25% of the *fus3*Δ cells overexpressing Bni1p-GFP, multiple actin-containing projections were observed (Fig. 7 C). Multi-projection shmoos were never observed in the wild-type strain overexpressing Bni1p-

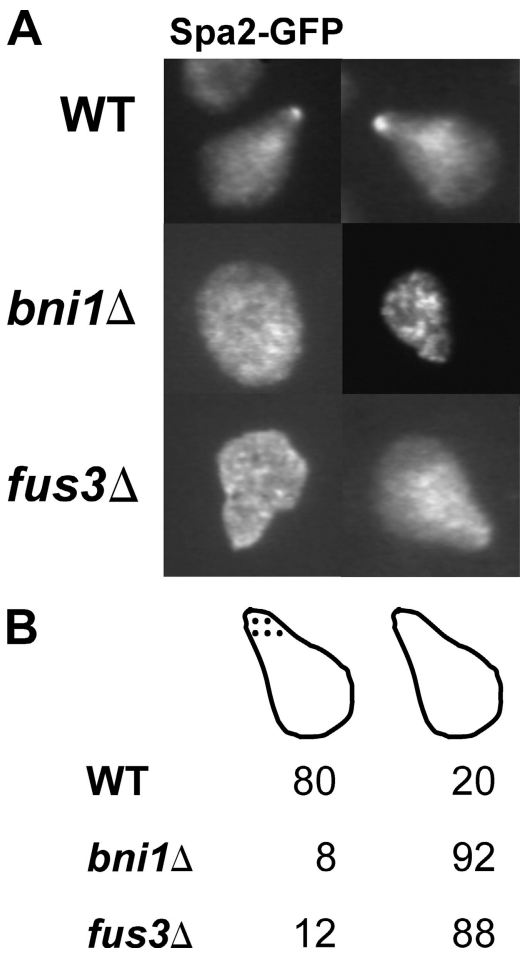

Figure 6. **Spa2p does not localize to the shmoo tips in *fus3* and *bni1* mutants.** (A) *WT* (EY699), *bni1*Δ (MY8188), and *fus3*Δ (EY700) cells transformed with p426S2G (expressing Spa2p-GFP) were induced with pheromone for 2 h, fixed with formaldehyde, and processed for immunofluorescence. Rabbit polyclonal anti-GFP antibody (from CLONTECH Laboratories, Inc.) was used at 1:25 dilution in PBS-BSA. (B) Cells were scored for GFP-Spa2p localization at the shmoo tip ($n > 100$).

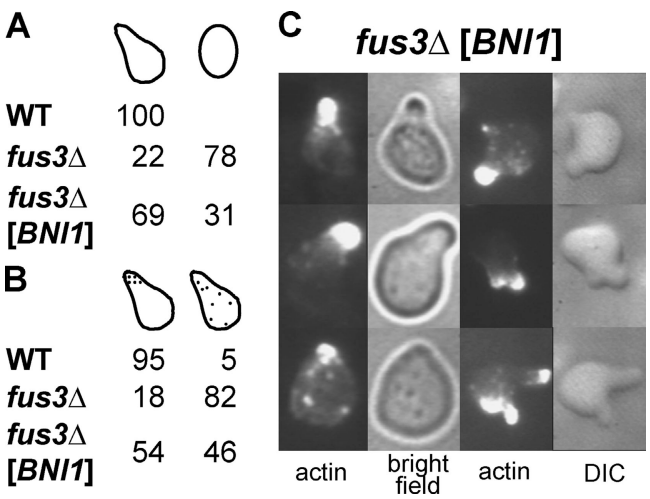

Figure 7. **Overexpression of *BNI1* suppresses the actin polarization and shmooing defect of a *fus3* mutant.** (A) *BNI1* expression was induced for 2 h with galactose and then pheromone was added for another 2 h to either *WT* (EY699), *fus3*Δ (EY700), or *fus3*Δ p*GAL-BNI1* (MY8196). Cells were fixed and examined by differential interference contrast or brightfield microscopy to determine whether they had formed shmoos. (B) The same strains as in A were stained with rhodamine-phalloidin and examined by fluorescence microscopy to determine the localization of actin ($n > 200$). (C) Representative cells in which overexpression of Bni1p has restored actin localization. Examples of cells with aberrant multiple shmoo projections are shown in the right-most panels.

GFP. Presumably, multiple sites of polarization arise because the Bni1p-dependent actin localization is uncoupled from the spatial signal defined by the site of receptor activation.

Although Bni1-GFP overexpression suppressed the *fus3*Δ polarization defect, in these cells, Bni1-GFP was not detected at the shmoo tips. Possibly, the small amount of Bni1p-GFP at the ends of the actin cables was too faint to be detected above the background fluorescence. Presumably, increasing the level of Bni1p raises it above a critical concentration for actin cable assembly at the shmoo tip, whereupon secondary interactions lead to actin cable clustering.

Next, we determined whether overexpression of Bni1p suppressed the *fus3*Δ cell fusion defect. To measure cell fusion, we performed matings with a *fus1 fus2* double mutant and determined the number of defective zygotes (residual septum between the cells and two nuclei; Fig. 8). Under these conditions, *fus3*Δ mutants exhibited a very strong mating defect; only 6% of mating pairs completed cell fusion. In contrast, 89% of zygotes formed by mating the *fus1 fus2* double mutant with the wild type completed cell fusion. When Bni1p was overexpressed, the cell fusion defect was suppressed more than fivefold; 32% of the zygotes completed cell fusion. Thus, at least part of the cell fusion defect of a *fus3*Δ mutant is associated with the defect in Bni1p-dependent polarization.

Simultaneous ablation of the preexisting bud site as well as the Far1p-dependent chemotropic pathway also results in cells that do not form projections (Nern and Arkowitz, 2000a). Nevertheless, such cells do show polarized growth, suggesting that a third pathway is responsible for cell polarization (Nern and Arkowitz, 2000a). To explore the contribution of Fus3p to polarized growth, we used differentially labeled Con A to distinguish the sites of cell wall growth (Nern and Arkowitz, 2000a). Mitotic cells were first labeled with FITC-Con A to mark the preexisting cell wall, then treated with pheromone, and finally labeled with TRITC-Con A to mark the sites of new growth (Fig. 9). We used a *fus3*Δ *cln3*Δ double mutant to suppress the cell cycle arrest defect (Elion et al., 1991b). Both the wild-type and *cln3*Δ mutant cells showed prominent polarized surface growth with new cell wall deposition occurring in one region with little overlap between the new and the old cell surfaces. In contrast, both the *fus3*Δ *cln3*Δ mutant and the *bni1*Δ mutant showed completely overlapping TRITC and FITC signals with no single site of new cell surface growth. We conclude that Fus3p, like Bni1p, is required for polarized growth in response to pheromone.

Discussion

Here, we report that the formin protein Bni1p is a substrate of the MAPK Fus3p in vitro, and the phosphorylation of

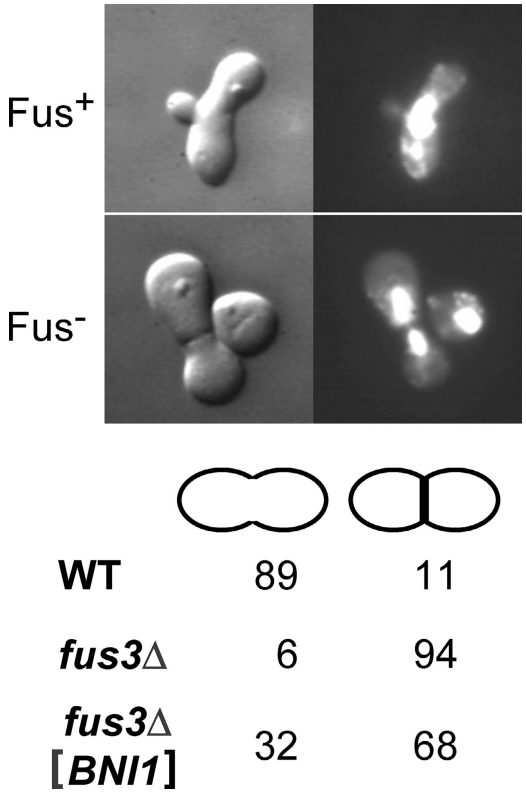

Figure 8. **Overexpression of *BNI1* suppresses the cell fusion defect of a *fus3* mutant.** *WT* (EY699), *fus3*Δ (EY700), and *fus3*Δ p*GAL-BNI1* (MY8196) cells were mated to a *MAT*α *fus1fus2* (MY1814) double mutant for 6 h as described in the Materials and methods. Cells were then fixed with methanol/acetic acid, stained with DAPI, and scored for the appearance of a septum (by differential interference contrast microscopy) and for the number and location of the nuclei (by fluorescence microscopy). Zygotes were scored as having a cell fusion defect based on the presence of a septum separating two unfused nuclei ($n > 100$).

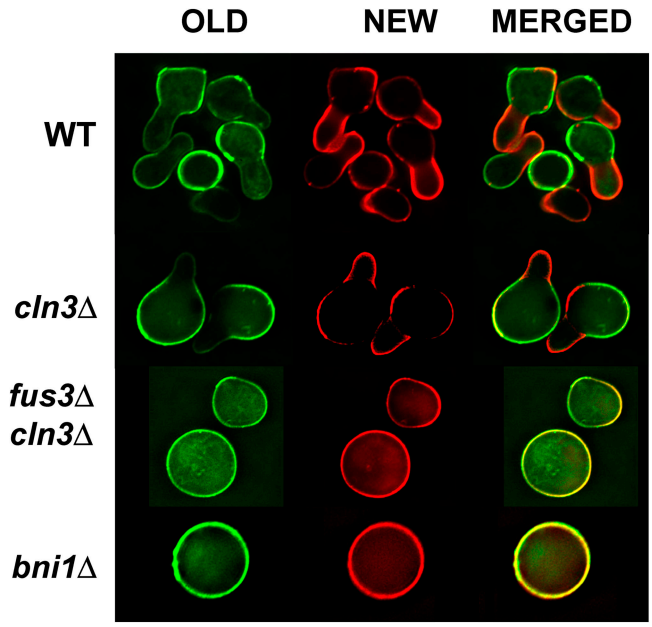

Figure 9. **New cell wall growth is not polarized in a *fus3* mutant.** WT (EY699), *cln3*Δ (MY5802), *fus3*Δ*cln3*Δ (MY5801), and *bni1*Δ (MY8188) were labeled for old growth (green) and new growth (red) after pheromone treatment using FITC- and TRITC-labeled Con A. Cells were visualized and deconvolved using a DeltaVision microscope.

Bni1p is dependent on Fus3p in vivo, during the pheromone response. Moreover, during the pheromone response, the phenotypes of *fus3*Δ and *bni1*Δ mutants were similar with respect to actin and cell polarization, Kar9p and Spa2p localization, and microtubule alignment. Overexpression of Bni1p partially suppressed the polarization phenotypes of a *fus3* mutant, suggesting that Bni1p functions downstream of Fus3p to promote these processes. Overexpression of Bni1p also partially suppressed the *fus3* cell fusion defect, suggesting that activation of Bni1p is one of the primary functions of Fus3p in cell fusion. Finally, a mutant form of Gpa1p that is defective for binding Fus3p conferred similar phenotypes, albeit weaker, suggesting that Fus3p regulation of Bni1p during pheromone signaling is partially dependent on the interaction between Fus3p and Gpa1p.

In the current model for cell polarization during mating, the interaction of Far1p with free Gβγ subunit at the cortex is thought to be the key signal for polarity establishment. By binding to Far1p, Cdc24p (and thus Cdc42p) would be targeted to the free Gβγ subunit, overriding the preexisting cortical cue for polarization at the bud site (Butty et al., 1998; Nern and Arkowitz, 1999, 2000b; Shimada et al., 2000). However, this model does not entirely explain the basis of pheromone-induced polarization. First, Far1p is not required for polarization; in the absence of Far1p, projections do form at the preexisting bud site. Second, although strains simultaneously containing a mutant form of Cdc24p unable to bind to Far1p (*cdc24-m1*) and defective for the cortical bud site cue (*bud1*Δ) are unable to form shmoo projections, they are still able to undergo polarized growth (Nern and Arkowitz, 2000a). Proteins required for polarized growth, such as Spa2p, still localize to the growth region, although their localization is unstable. These data imply that another signal establishes cell polarization in response to pheromone. We found that *fus3* mutants were unable to establish even residual polarized growth during pheromone signaling, suggesting that Fus3p signaling is required to establish or maintain polarized cell growth in response to pheromone.

Our finding that Bni1p was mislocalized in the *fus3* mutant and that Bni1p overexpression suppressed the *fus3* defects supports a model in which Bni1p acts downstream of Fus3p for cell polarization. Given the in vitro phosphorylation data, it is most likely that Bni1p is directly phosphorylated by Fus3p in vivo. However, it remains formally possible that a downstream event is responsible for activation. Regardless of mechanism, activation of Bni1p would facilitate its ability to nucleate actin assembly at the site of the incipient shmoo projection. Bni1p might be either more stably associated with the cortex at that site, be more active for actin assembly, or interact more strongly with other proteins required for assembly. One possible target for regulation is the FH3 domain, which has been implicated in the localization of the Fus1 formin (as well as other formins) in the fission yeast *Schizosaccharomyces pombe* (Petersen et al., 1998).

It is thought that small differences in pheromone receptor activity are amplified and reinforced to generate the asym-

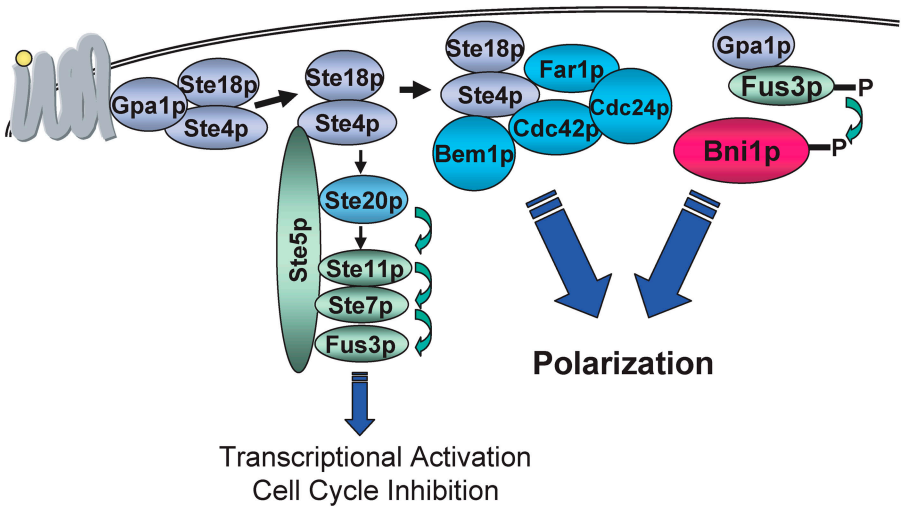

Figure 10. **A model of Fus3p-dependent Bni1p activation.** Upon pheromone binding to its receptor, a heterotrimeric G protein dissociates. The Gβγ subunit, comprised of Ste4p and Ste18p, respectively, is required for activation of the MAPK module and for recruitment of Far1p, Cdc42p, and Cdc24p, which establish the site for the future shmoo projection. Free Gpa1p recruits phosphorylated active Fus3p back to the site of receptor activation, facilitating the local Fus3p-dependent phosphorylation of Bni1p and leading to the stable localization of Bni1p at the incipient shmoo site. Bni1p then nucleates actin assembly and other functions required for polarization of the cell toward the pheromone gradient.

metry that determines where the shmoo projection will form (Ayscough and Drubin, 1998; Arkowitz, 1999). The cortical site of receptor activation has been thought to be marked solely by the appearance of free Gβγ subunit. However, phosphorylated Fus3p also interacts with the Gα subunit, Gpa1p (Metodiev et al., 2002). Therefore, the recruitment of activated Fus3p by Gpa1p may also contribute to recognition of the cortical site of receptor activation. Active Fus3p recruited to the cortex near the active receptor would lead to local activation of Bni1p, facilitating localized actin assembly and polarized growth. Thus, one model for the Gpa1p–Fus3p–Bni1p interaction is that it serves as an additional cortical cue in determining the site of shmoo formation.

In this view, there would be two "pathways" for cell polarization in response to pheromone (Fig. 10). In one path, the Gβγ interaction with Far1p recruits Cdc24p, Cdc42p, and Bem1p to the incipient shmoo site, away from the bud site. In the second path, activated Fus3p, presumably in association with Gpa1p, would localize Bni1p and the polarisome complex to the incipient shmoo site. Cells would need both pathways to respond correctly to a pheromone gradient. However, the two pathways need not be mutually exclusive, and other pathways may also contribute.

During chemotropic mating, cells orient growth along pheromone gradients (Schrick et al., 1997). During "default mating," cells cannot sense the gradient (as happens in an excess of pheromone) and instead use the bud site to initiate polarized growth (Dorer et al., 1997). *fus3* mutants show defects in both the default and the chemotropic mating pathways (Schrick et al., 1997). The *fus3* chemotropic defect is weaker than that seen for mutations affecting the receptor and Gβγ, consistent with a model in which Gβγ recruitment plays a primary role in determining the site of polarization. Presumably, the *fus3* chemotropic defect results from the inability of Bni1p to localize; the failure to polarize at a unique site might allow *fus3* cells to mate with nonsignaling partners via adventitious contacts.

The $gpa1^{K21E\ R22E}$ mutation also causes a defect in chemotropic mating (Metodiev et al., 2002), consistent with the idea that Gpa1p helps localize active Fus3p at the shmoo tip. In the $gpa1^{K21E\ R22E}$ mutant, the localization of Fus3p at the shmoo tip was altered but not abolished (Metodiev et al., 2002). Active Fus3p would still be present to activate Bni1p, although possibly with reduced efficiency, consistent with the relatively mild defects of the $gpa1^{K21E\ R22E}$ mutant in actin polarization, shmoo formation, and Bni1p localization. The stronger defect in Kar9p localization and microtubule orientation may indicate that Gpa1p interacts with other proteins affecting microtubule function independent of Bni1p and/or Fus3p.

Several mutations cause defects in both cell polarity and cell fusion. Before cell fusion, vesicles localize to the shmoo tip, and these vesicles are thought to carry cargo required for the localized degradation of the cell walls and subsequent membrane fusion (Gammie et al., 1998). Accordingly, we expect defects in actin polarization and localized secretion to cause defects in cell fusion. Bni1p overexpression partially suppressed the *fus3* mutant polarization and cell fusion phenotypes. Most likely, suppression occurs because, through mass action, overexpressed Bni1p assembles at sites of activated receptor where there are other proteins with which it interacts, and which also may be needed for Bni1p activation (e.g., Cdc42p). There are several possible explanations for incomplete suppression. First, overexpression of Bni1p mutant may not restore stable localization to the shmoo tip. Second, overexpression led to the appearance of abnormal shmoos with multiple projections. Possibly, part of the requirement for two pathways in cell polarization is to ensure that only a single site is chosen for polarization. Finally, although these results strongly imply that Fus3p acts through Bni1p for cell fusion, it is also likely that Fus3p is required for yet more functions in mating, in addition to the known roles.

Materials and methods

General yeast techniques

Yeast media and general techniques were described previously (Rose et al., 1990). In all cases, yeast strains were grown at 30°C. When inducing with galactose, cells were first grown overnight in synthetic complete (SC) media containing 2% raffinose, and then grown to early logarithmic phase in 2% raffinose + 2% galactose. Synthetic α factor (Syn/Seq Facility, Princeton University, Princeton, NJ) was added to 10 μg/ml. Transformations were done as described previously (Gietz and Woods, 2002). Yeast strains and bacterial plasmids are listed in Table I and Table II. To construct the *gpa1*Δ::URA3, pDSB138 was digested with EcoRI and was cotransformed

Table I. **Yeast strains**

Strain	Genotype
EY699	*MAT***a** *ura3-1 his3-11,15 leu2-3,112 trp1-1 ade2-1 can1-100 GAL+*
EY700	*MAT***a** *fus3-6*Δ::*LEU2 ura3-1 his3-11,15 leu2-3,112 trp1-1 ade2-1 can1-100 GAL+*
MY5801	*MAT***a** *fus3-6*Δ::*LEU2 cln3::ura3FOA*^{r} *ura3-1 his3-11,15 leu2-3,112 trp1-1 ade2-1 can1-100 GAL+*
MY5802	*MAT***a** *cln3*::*ura3FOA*^{r} *ura3-1 his3-11,15 leu2-3,112 trp1-1 ade2-1 can1-100 GAL+*
MY8188	*MAT***a** *bni1*Δ::*URA3 ura3 his3-11,15 leu2-3,112 trp1-1 ade2-1 can1-100 GAL+*
MY8193	*MAT***a** *gpa1*Δ::*URA3 ura3 his3-11,15 leu2-3,112 trp1-1 ade2-1 can1-100 GAL+* (MDB107)
JY429	*MAT*α *fus1*Δ *fus2-*Δ*3 ura3-52 trp1-*Δ*1*
MY8189	*MAT***a** *ura3-1 his3-11,15 leu2-3,112 trp1-1 ade2-1 can1-100 GAL+* (pMR3465)
MY7494	*MAT***a** *fus3-6*Δ::*URA3 ura3-1 his3-11,15 leu2-3,112 trp1-1 ade2-1 can1-100 GAL+* (pMR5049) (pMR3465)
MY8194	*MAT***a** *gpa1*Δ::*URA3 ura3-1 his3-11,15 leu2-3,112 trp1-1 ade2-1 can1-100 GAL+* (MDB107) (pMR3465)
MY8195	*MAT***a** *ura3-1 his3-11,15 leu2-3,112 trp1-1 ade2-1 can1-100 GAL+* (p1955)
MY8196	*MAT***a** *fus3-6*Δ::*LEU2 ura3 his3-11,15 leu2-3,112 trp1-1 ade2-1 can1-100 GAL+* (p1955)
MY8351	*MAT***a** *gpa1*Δ::*ura3*::*HIS3 ura3-1 his3-11,15 leu2-3,112 trp1-1 ade2-1 can1-100 GAL+* (MDB107) (pUH7)
MY8352	*MAT***a** *gpa1*Δ::*HIS3 ura3-1 his3-11,15 leu2-3,112 trp1-1 ade2-1 can1-100 GAL+* (MDB107) (p1955)
MY8341	*MAT***a** *fus3-6*Δ::*LEU2 ura3-1 his3-11,15 leu2-3,112 trp1-1 ade2-1 can1-100 GAL+* (pMR4937)
MY8342	*MAT***a** *fus3-6*Δ::*LEU2 ura3-1 his3-11,15 leu2-3,112 trp1-1 ade2-1 can1-100 GAL+* (pMR4938)
MY8343	*MAT***a** *ura3-1 his3-11,15 leu2-3,112 trp1-1 ade2-1 can1-100 GAL+* (p426S2G)
MY8344	*MAT***a** *fus3-6*Δ::*LEU2 ura3-1 his3-11,15 leu2-3,112 trp1-1 ade2-1 can1-100 GAL+* (p426S2G)

Strains EY699, EY700, and JY429 are from the laboratory of G. Fink (Massachusetts Institute of Technology, Cambridge, MA). Otherwise, strains were constructed for this work.

into EY699 with pMDB107, resulting in strain MY8193. The *bni1*Δ::*URA3* strain was made by cutting p321 (Evangelista et al., 1997) with HindIII and XhoI and transforming into EY699, resulting in strain MY8188.

Matings

Microscopic analysis of zygotes was performed as described previously (Rose et al., 1990). Briefly, MAT**a** and MATα cells in early log phase of growth were mixed on 0.45-μm nitrocellulose filter discs (Millipore), transferred to a YEPD plate, and incubated for 6 h. Cells were rinsed off the filter, centrifuged at 2,000 rpm for 5 min, and resuspended in a 3:1 ratio of methanol/acetic acid for 30 min on ice. Cells were washed twice with PBS and stained with DAPI at 1 mg/ml in PBS for 5 min at RT, and were washed three times with PBS.

Microscopy

For most experiments, cells were visualized by differential interference contrast and fluorescence microscopy (Axiophot; Carl Zeiss MicroImaging, Inc.) using a 100× Neofluar objective and appropriate filter cubes. Images were acquired with a video camera (C2400-08 SIT; Hamamatsu Corporation), processed using an Omnex Image processing unit (Imagen), and captured to computer disk with an image capture board (Scion Corporation). For cell surface growth experiments, images were acquired using a DeltaVision microscope workstation (Applied Precision) based on a microscope (Eclipse TE600; Nikon), using a 100× objective and a CCD camera (CoolSNAP HQ™; Roper Scientific). Where appropriate, Adobe Photoshop® was used to optimize image contrast.

Immunological techniques

Actin was visualized using rhodamine-phalloidin (Molecular Probes, Inc.) as described previously (Rose et al., 1990). Briefly, 5 ml of cells were induced with pheromone and fixed with 4% formaldehyde for 30 min at 30°C. Cells were washed and resuspended in 100 μl PBS. 50 μl of cells were added to 25 μl rhodamine-phalloidin and incubated at RT for 5 min. Cells were washed three times in PBS.

For visualizing GFP-tagged proteins by immunofluorescence, cells were fixed with 4% formaldehyde (for 1 h at 30°C) and converted to spheroplasts (25 μg/ml Zymolyase 100,000T [ICN Biomedicals] and 25 mM β-mercaptoethanol for 45 min at 30°C) as described previously (Rose et al., 1990). Polyclonal anti-GFP antibody (CLONTECH Laboratories, Inc.) was used at 1:25 dilution in 10 mg/ml PBS-BSA. Fluorescein-conjugated goat anti–rabbit antiserum (Boehringer) was used at 1:100 dilution. For visualizing tubulin, rat monoclonal anti-tubulin antibody YOL1/34 (Sera-lab) was used at 1:2 dilution in 10 mg/ml PBS-BSA. Fluorescein-conjugated goat anti–rat antiserum (Boehringer) was used at 1:25 dilution.

For the FITC- and TRITC-Con A (Sigma-Aldrich) labeling experiments (Nern and Arkowitz, 2000a), cells were grown in the SC complete media

Table II. **Plasmids and bacterial strains**

Strain	Genotype/description	Source
pMR4937	FLAG-*FUS3 URA3 CEN3 ARS1 AMP*^{R}	
pMR4938	FLAG-*FUS3*^{Q93G} *URA3 CEN3 ARS1 AMP*^{R}	
pMR5049	FLAG-*FUS3*^{Q93G} *HIS3 CEN3 ARS1 AMP*^{R}	
pMR3465	P_{GAL1}-*GFP-KAR9 LEU2 CEN4 ARS1 AMP*^{R}	
p321	*BNI1* disruption construct	Dr. C. Boone, University of Toronto, Toronto, Canada
p1955	2μ P_{GAL1}-HA-*BNI1-GFP URA3 CEN4 ARS1 AMP*^{R}	Dr. C. Boone
p426S2G	2μ *SPA2-GFP URA3 ARS1 AMP*^{R}	Dr. R. Arkowitz, CNRS, Nice, France
DSB138	*GPA1* disruption construct	
MDB107	*gpa1*$^{K21E\ R22E}$ *TRP1 CEN4 ARS1 AMP*^{R}	
UH7	*ura3*::*LEU2 KAN*^{R} *AMP*^{R}	Dr. F. Cross, The Rockefeller University, New York, NY

Plasmids were from the laboratories of M.D. Rose, D. Stone, or as indicated.

(pH 3.5) for 2 h. Cells were spun down and resuspended in 1 ml FITC-Con A (0.1 mg/ml), and were incubated in the dark for 10 min. Cells were washed three times, resuspended in prewarmed media plus α-factor, and incubated for 2.5 h. TRITC-Con A labeling was performed as for FITC-Con A. After washing, cells were fixed in 4% formaldehyde for 15 min.

To determine Bni1p levels, 100-ml cultures in early log phase were grown in SC-URA raffinose + 2% galactose for 2 h and treated with or without α-factor for an additional 2 h. Protein extracts were made as described previously (Ohashi et al., 1982). Extract protein levels were normalized by measurement of the OD_{280}. HA epitope antibody 12CA5 was used at 1:2,500 dilution, and HRP-conjugated goat anti–mouse secondary antibody was used at 1:2,500 dilution (Amersham Biosciences).

For immunoprecipitation (IP) experiments, cells were collected and resuspended in lysis buffer (50 mM Tris-HCl, pH 7.5, 150 mM NaCl, 5 mM EDTA, 1% NP-40, 15 mM pNPP, 15 mM $Na_2H_2P_2O_7$, 25 mM NaF, 0.25 mM orthovanadate, 1 mM PMSF, and 1 mM DTT; Zhan et al., 1997) with the addition of a cocktail of protease inhibitors ([μg/ml] 5 chymostatin, 5 leupeptin, 5 aprotinin, and 5 pepstatin). Acid-washed glass beads (Biospec Products, Inc.) were added and cells were vortexed five times for 1 min followed by 1 min on ice. Unbroken cells were removed by 3,000-rpm centrifugation for 10 min. Supernatants were cleared by centrifugation (15 min at 11,000 rpm). For anti-FLAG IPs, 30 μl of anti-FLAG M2 Affinity Gel (Sigma-Aldrich) was used. For anti-HA IPs, a 1:150 dilution of 12CA5 antibody was used with a 30-μl slurry of Protein G Plus Agarose (Santa Cruz Biotechnology, Inc.).

In vitro kinase assay

For FLAG-Fus3p, 200-ml cultures of early logarithmic cells were induced for 45 min with α-factor. For HA-Bni1p, 150 ml of early logarithmic cells was used. In both cases, extracts were prepared in 1 ml lysis buffer and tagged proteins were bound to the affinity gel. Bound proteins were resuspended in kinase buffer ([mM] 25 Hepes, pH 7.2, 15 $MgCl_2$, 5 EGTA, 1 DTT, 0.1 orthovanadate, 15 pNPP, and 1 PMSF; Zhan et al., 1997). Purified Fus3p and Bni1p were resuspended in 20 μl kinase buffer. Each reaction contained 5 μl Fus3p, 10 μM ATP, and 3 μl γ[^{32}P]phenethyl-ATP. γ[^{32}P]phenethyl-ATP was prepared from phenethyl-ADP (provided by K. Shah, Novartis, San Diego, CA; and K. Shokat, University of California, San Francisco, San Francisco, CA) using nucleoside diphosphate kinase by the following method. A 200-μl slurry (1:1) of IDA Co^{2+} Sepharose beads (Sigma-Aldrich) and HBS (150 mM NaCl and 10 mM Hepes, pH 7.4) was added to a mini-column constructed from a 1-ml pipette tip. 200 μg nucleoside diphosphate kinase was added to the column and washed with 1 ml HBS. 7,000 Ci/mmol [^{32}P]ATP (ICN Biomedicals) was added to the column and washed twice with 1 ml HBS + 5 mM $MgCl_2$. Next, 8 μl of 1 mM phenethyl-ADP in 32 μl HBS + 5 mM $MgCl_2$ was added to the column. Finally, 250 μl HBS + 5 mM $MgCl_2$ was used to elute the labeled [^{32}P] phenethyl-ATP (protocol from J. Blethrow and K. Shokat, University of California, San Francisco, San Francisco, CA). To measure Bni1p phosphorylation, 10 μl purified Bni1p was added to the experiment. In some cases, the inhibitor 1-Na PP1 was added to 10 μM (K. Shokat). Reactions proceeded for 30 min at 30°C and were stopped by the addition of SDS-PAGE buffer and boiling for 10 min. Proteins were resolved by SDS-PAGE. The gel was fixed for 1 h in 10% methanol, 10% acetic acid, and 0.5% phosphoric acid, and then for 30 min in 10% methanol and 10% acetic acid. The gel was dried for 1 h and exposed to x-ray film or to a PhosphorImager screen, and was scanned using Storm® software (Molecular Dynamics).

Metabolic cell labeling

For in vivo ^{32}P labeling, 100-ml cultures were grown to 1.2×10^7 cells/ml in minimal media, transferred to growth in low phosphate media with galactose for 2 h, and then were collected and resuspended in no-phosphate media containing galactose and α-factor. After 60 min, 1 mCi carrier-free [^{32}P]orthophosphate (ICN Biomedicals) was added and cells were grown for an additional 30 min. Cells were harvested, and extracts and immunoprecipitation were performed as described above.

We thank Rob Arkowitz, Charlie Boone, Fred Cross, and Gerry Fink for strains and plasmids. We particularly thank K. Shah, J. Belthrow, and K. Shokat for providing ATP analogues and protocols. We are grateful to Eric Phizicky for providing the GST fusion library.

This work was supported by National Institutes of Health grant GM37739 to M.D. Rose and National Science Foundation grant MCB-0218081 to D. Stone. D. Matheos was supported by a National Institutes of Health predoctoral training grant as well as by the New Jersey Cancer Commission Fund for Research Fellowship.

Submitted: 15 September 2003
Accepted: 27 February 2004

References

Arkowitz, R.A. 1999. Responding to attraction: chemotaxis and chemotropism in *Dictyostelium* and yeast. *Trends Cell Biol.* 9:20–27.

Ayscough, K.R., and D.G. Drubin. 1998. A role for the yeast actin cytoskeleton in pheromone receptor clustering and signalling. *Curr. Biol.* 8:927–930.

Bishop, A.C., J.A. Ubersax, D.T. Petsch, D.P. Matheos, N.S. Gray, J. Blethrow, E. Shimizu, J.Z. Tsien, P.G. Schultz, M.D. Rose, et al. 2000. A chemical switch for inhibitor-sensitive alleles of any protein kinase. *Nature.* 407:395–401.

Butty, A.C., P.M. Pryciak, L.S. Huang, I. Herskowitz, and M. Peter. 1998. The role of Far1p in linking the heterotrimeric G protein to polarity establishment proteins during yeast mating. *Science.* 282:1511–1516.

Chenevert, J., N. Valtz, and I. Herskowitz. 1994. Identification of genes required for normal pheromone-induced cell polarization in *Saccharomyces cerevisiae*. *Genetics.* 136:1287–1296.

Choi, K.Y., B. Satterberg, D.M. Lyons, and E.A. Elion. 1994. Ste5 tethers multiple protein kinases in the MAP kinase cascade required for mating in *S. cerevisiae*. *Cell.* 78:499–512.

Cook, J.G., L. Bardwell, and J. Thorner. 1997. Inhibitory and activating functions for MAPK Kss1 in the *S. cerevisiae* filamentous-growth signalling pathway. *Nature.* 390:85–88.

Dong, Y., D. Pruyne, and A. Bretscher. 2003. Formin-dependent actin assembly is regulated by distinct modes of Rho signaling in yeast. *J. Cell Biol.* 161: 1081–1092.

Dorer, R., C. Boone, T. Kimbrough, J. Kim, and L.H. Hartwell. 1997. Genetic analysis of default mating behavior in *Saccharomyces cerevisiae*. *Genetics.* 146: 39–55.

Elion, E.A., P.L. Grisafi, and G.R. Fink. 1990. FUS3 encodes a cdc^{2+}/CDC28-related kinase required for the transition from mitosis into conjugation. *Cell.* 60:649–664.

Elion, E.A., J.A. Brill, and G.R. Fink. 1991a. Functional redundancy in the yeast cell cycle: FUS3 and KSS1 have both overlapping and unique functions. *Cold Spring Harb. Symp. Quant. Biol.* 56:41–49.

Elion, E.A., J.A. Brill, and G.R. Fink. 1991b. FUS3 represses CLN1 and CLN2 and in concert with KSS1 promotes signal transduction. *Proc. Natl. Acad. Sci. USA.* 88:9392–9396.

Elion, E.A., B. Satterberg, and J.E. Kranz. 1993. FUS3 phosphorylates multiple components of the mating signal transduction cascade: evidence for STE12 and FAR1. *Mol. Biol. Cell.* 4:495–510.

Evangelista, M., K. Blundell, M.S. Longtine, C.J. Chow, N. Adames, J.R. Pringle, M. Peter, and C. Boone. 1997. Bni1p, a yeast formin linking cdc42p and the actin cytoskeleton during polarized morphogenesis. *Science.* 276:118–122.

Evangelista, M., D. Pruyne, D.C. Amberg, C. Boone, and A. Bretscher. 2002. Formins direct Arp2/3-independent actin filament assembly to polarize cell growth in yeast. *Nat. Cell Biol.* 4:260–269.

Fujimura, H. 1990. Molecular cloning of the DAC2/FUS3 gene essential for pheromone-induced G1-arrest of the cell cycle in *Saccharomyces cerevisiae*. *Curr. Genet.* 18:395–400.

Fujimura, H.A. 1992. The DAC2/FUS3 protein kinase is not essential for transcriptional activation of the mating pheromone response pathway in *Saccharomyces cerevisiae*. *Mol. Gen. Genet.* 235:450–452.

Fujiwara, T., K. Tanaka, A. Mino, M. Kikyo, K. Takahashi, K. Shimizu, and Y. Takai. 1998. Rho1p-Bni1p-Spa2p interactions: implication in localization of Bni1p at the bud site and regulation of the actin cytoskeleton in *Saccharomyces cerevisiae*. *Mol. Biol. Cell.* 9:1221–1233.

Gammie, A.E., V. Brizzio, and M.D. Rose. 1998. Distinct morphological phenotypes of cell fusion mutants. *Mol. Biol. Cell.* 9:1395–1410.

Gartner, A., K. Nasmyth, and G. Ammerer. 1992. Signal transduction in *Saccharomyces cerevisiae* requires tyrosine and threonine phosphorylation of FUS3 and KSS1. *Genes Dev.* 6:1280–1292.

Gehrung, S., and M. Snyder. 1990. The SPA2 gene of *Saccharomyces cerevisiae* is important for pheromone-induced morphogenesis and efficient mating. *J. Cell Biol.* 111:1451–1464.

Gietz, R.D., and R.A. Woods. 2002. Transformation of yeast by lithium acetate/single-stranded carrier DNA/polyethylene glycol method. *Methods Enzymol.* 350:87–96.

Goehring, A.S., D.A. Mitchell, A.H. Tong, M.E. Keniry, C. Boone, and G.F. Sprague, Jr. 2003. Synthetic lethal analysis implicates Ste20p, a p21-activated protein kinase, in polarisome activation. *Mol. Biol. Cell.* 14:1501–1516.

Hwang, E., J. Kusch, Y. Barral, and T.C. Huffaker. 2003. Spindle orientation in *Saccharomyces cerevisiae* depends on the transport of microtubule ends along polarized actin cables. *J. Cell Biol.* 161:483–488.

Imamura, H., K. Tanaka, T. Hihara, M. Umikawa, T. Kamei, K. Takahashi, T. Sasaki, and Y. Takai. 1997. Bni1p and Bnr1p: downstream targets of the Rho family small G-proteins which interact with profilin and regulate actin cytoskeleton in *Saccharomyces cerevisiae*. *EMBO J.* 16:2745–2755.

Lee, L., S.K. Klee, M. Evangelista, C. Boone, and D. Pellman. 1999. Control of mitotic spindle position by the *Saccharomyces cerevisiae* formin Bni1p. *J. Cell Biol.* 144:947–961.

Liu, Y., K. Shah, F. Yang, L. Witucki, and K.M. Shokat. 1998. Engineering Src family protein kinases with unnatural nucleotide specificity. *Chem. Biol.* 5:91–101.

Marsh, L., and M.D. Rose. 1997. The pathway of cell and nuclear fusion during mating in *S. cerevisiae*. *In* The Molecular and Cellular Biology of the Yeast *Saccharomyces cerevisiae*. J.R. Pringle, J.R. Broach, and E.W. Jones, editors. Cold Spring Harbor Laboratory, Cold Spring Harbor, NY. 827–888.

Martzen, M.R., S.M. McCraith, S.L. Spinelli, F.M. Torres, S. Fields, E.J. Grayhack, and E.M. Phizicky. 1999. A biochemical genomics approach for identifying genes by the activity of their products. *Science.* 286:1153–1155.

Matheos, D. 2003. Analysis of Fus3p and its requirements during cell fusion. *In* Molecular Biology. Princeton University, Princeton, NJ. 135 pp.

Metodiev, M.V., D. Matheos, M.D. Rose, and D.E. Stone. 2002. Regulation of MAPK function by direct interaction with the mating-specific Gα in yeast. *Science.* 296:1483–1486.

Miller, R.K., D. Matheos, and M.D. Rose. 1999. The cortical localization of the microtubule orientation protein, Kar9p, is dependent upon actin and proteins required for polarization. *J. Cell Biol.* 144:963–975.

Nern, A., and R.A. Arkowitz. 1999. A Cdc24p-Far1p-Gβγ protein complex required for yeast orientation during mating. *J. Cell Biol.* 144:1187–1202.

Nern, A., and R.A. Arkowitz. 2000a. G proteins mediate changes in cell shape by stabilizing the axis of polarity. *Mol. Cell.* 5:853–864.

Nern, A., and R.A. Arkowitz. 2000b. Nucleocytoplasmic shuttling of the Cdc42p exchange factor Cdc24p. *J. Cell Biol.* 148:1115–1122.

Ohashi, A., J. Gibson, I. Gregor, and G. Schatz. 1982. Import of proteins into mitochondria. The precursor of cytochrome c1 is processed in two steps, one of them heme-dependent. *J. Biol. Chem.* 257:13042–13047.

Ozaki-Kuroda, K., Y. Yamamoto, H. Nohara, M. Kinoshita, T. Fujiwara, K. Irie, and Y. Takai. 2001. Dynamic localization and function of Bni1p at the sites of directed growth in *Saccharomyces cerevisiae*. *Mol. Cell. Biol.* 21:827–839.

Petersen, J., O. Nielsen, R. Egel, and I.M. Hagan. 1998. FH3, a domain found in formins, targets the fission yeast formin Fus1 to the projection tip during conjugation. *J. Cell Biol.* 141:1217–1228.

Pruyne, D., M. Evangelista, C. Yang, E. Bi, S. Zigmond, A. Bretscher, and C. Boone. 2002. Role of formins in actin assembly: nucleation and barbed-end association. *Science.* 297:612–615.

Rose, M.D., F. Winston, and P. Hieter. 1990. Methods of Yeast Genetics. Cold Spring Harbor Laboratory, Cold Spring Harbor, NY. 198 pp.

Sagot, I., S.K. Klee, and D. Pellman. 2002a. Yeast formins regulate cell polarity by controlling the assembly of actin cables. *Nat. Cell Biol.* 4:42–50.

Sagot, I., A.A. Rodal, J. Moseley, B.L. Goode, and D. Pellman. 2002b. An actin nucleation mechanism mediated by Bni1 and profilin. *Nat. Cell Biol.* 4:626–631.

Schrick, K., B. Garvik, and L.H. Hartwell. 1997. Mating in *Saccharomyces cerevisiae*: the role of the pheromone signal transduction pathway in the chemotropic response to pheromone. *Genetics.* 147:19–32.

Shah, K., Y. Liu, C. Deirmengian, and K.M. Shokat. 1997. Engineering unnatural nucleotide specificity for Rous sarcoma virus tyrosine kinase to uniquely label its direct substrates. *Proc. Natl. Acad. Sci. USA.* 94:3565–3570.

Sheu, Y.J., Y. Barral, and M. Snyder. 2000. Polarized growth controls cell shape and bipolar bud site selection in *Saccharomyces cerevisiae*. *Mol. Cell. Biol.* 20: 5235–5247.

Shimada, Y., M.P. Gulli, and M. Peter. 2000. Nuclear sequestration of the exchange factor Cdc24 by Far1 regulates cell polarity during yeast mating. *Nat. Cell Biol.* 2:117–124.

Sprague, G.F., and J.W. Thorner. 1994. Pheromone response and signal transduction during the mating process of *Saccharomyces cerevisiae*. *In* The Molecular and Cellular Biology of the Yeast *Saccharomyces*. J.R. Broach, J.R., Pringle, and E.W. Jones, editors. Cold Spring Harbor Laboratory, Cold Spring Harbor, NY. 657–744.

Tedford, K., S. Kim, D. Sa, K. Stevens, and M. Tyers. 1997. Regulation of the mating pheromone and invasive growth responses in yeast by two MAP kinase substrates. *Curr. Biol.* 7:228–238.

Valtz, N., M. Peter, and I. Herskowitz. 1995. FAR1 is required for oriented polarization of yeast cells in response to mating pheromones. *J. Cell Biol.* 131: 863–873.

Yin, H., D. Pruyne, T.C. Huffaker, and A. Bretscher. 2000. Myosin V orientates the mitotic spindle in yeast. *Nature.* 406:1013–1015.

Zhan, X.L., R.J. Deschenes, and K.L. Guan. 1997. Differential regulation of FUS3 MAP kinase by tyrosine-specific phosphatases PTP2/PTP3 and dual-specificity phosphatase MSG5 in *Saccharomyces cerevisiae*. *Genes Dev.* 11:1690–1702.